# Generation, Validation, and Utilization of a Three-Dimensional Pharmacophore Model for EP3 Antagonists

Rama K. Mishra[‡,†] and Jasbir Singh[‡,*,†]

deCODE Chemistry Incorporated, 2501 Davey Road, Woodridge, Illinois 60517

Studies reported here are aimed to investigate the important structural features that characterize the human EP$_3$ antagonists. Based on the knowledge of low-energy conformation of the endogenous ligand, the initial hit analogs were prepared. Subsequently, a ligand-based lead optimization approach using pharmacophore model generation was utilized. A 5-point pharmacophore using a training set of 19 compounds spanning the IC$_{50}$ data over 4-log order was constructed using the HypoGen module of Catalyst. Following pharmacophore customization, using a linear structure−activity regression equation, a six feature three-dimensional predictive pharmacophore model, P6, was built, which resulted in improved predictive power. The P6 model was validated using a test set of 11 compounds providing a correlation coefficient ($R^2$) of 0.90 for predictive versus experimental EP$_3$ IC$_{50}$ values. This pharmacophore model has been expanded to include diverse chemotypes, and the predictive ability of the customized pharmacophore has been tested.

## INTRODUCTION

Among the prostanoids, Prostaglandin E2 (PGE$_2$) preferentially binds to the EP family of receptors known as EP$_{1-4}$.[1] PGE$_2$, has been reported to have biphasic effect on the platelet response, as it potentiates platelet aggregation at low concentrations and inhibits this effect at higher concentrations.[2] Furthermore, studies using EP$_3$ knockout (KO) mice showed that the stimulatory effects of PGE$_2$ on platelet aggregation are exerted specifically through EP$_3$ receptors.[3] We have recently reported that the selective EP$_3$ receptor antagonists are expected to be antithrombotic agents without causing increased risk of bleeding.[4]

Several literature reports for the ligand design for seven transmembrane G protein-coupled receptors (GPCR) are derived from HTS campaigns,[5] based on privileged structures,[6] modifications of ligands reported in the literature for receptors of interest, and in silico design using homology models.[7] In this paper, we present the generation of initial leads that are based on the knowledge of endogenous ligand's low-energy conformation. In particular, we describe: (i) the generation of initial hypothesis for antagonist design; (ii) the approaches that have been used to build and validate pharmacophore model(s); and (iii) the utilization of an optimized pharmacophore model that resulted in the expansion and identification of novel, diverse chemotype-derived potent hEP$_3$ antagonists.

Comparison of PGE$_2$ (**1**) and a synthetic EP$_3$ selective agonist Sulprostone (**2**) clearly indicates tolerance of structural variation in the tail portion of the PGE$_2$ structure for binding to a hEP$_3$ receptor (Figure 1a). This suggests that changes to the cyclopentanoid portion might provide EP$_3$ antagonists. Compound **3** and related analogs[8] also support this notion. We hypothesize that, by appropriate choice of the core bearing the hydrophobic and anionic pharmacophoric appendages, it should be feasible to retain key features represented by the Sulprostone/PGE$_2$ for binding to the EP$_3$ receptor. We envisioned a cyclic core structure where the nonvicinal ring atoms bearing these two pharmacophoric features would overlap with the C7/C13 or C8/C14 atoms of PGE$_2$ and thus provide an approach for the design of new chemotypes. Furthermore, to provide an element of preorganization, we elected to utilize perisubstituted bicyclic as a basic building block for our chemotypes. This concept is depicted schematically in the Figure 2, which incorporates combined features of the endogenous ligand PGE2 (**1**), the potent and selective EP3 agonist Sulprostone (**2**), and cinnamic acid-based EP3 antagonist (**3**), thus providing a hairpin U-shaped motif for the putative small molecules. This analysis led to the synthesis of indole-derived analogs **4** and **5**, as the initial examples. As reported previously, these initial compounds showed very good activity in the hEP$_3$ receptor radioligand displacement assay with nM IC$_{50}$ (Figure 3) and were shown to exhibit full antagonism in the functional cellular assays.[7]

## COMPUTATIONAL METHODS FOR OVERLAY OF LIGANDS

The PGE$_2$ (**1**) and Sulprostone (**2**), the two known hEP$_3$ agonists, along with our initial hit (**5**) were minimized with MMFF94 using a conjugate gradient minimization algorithm with a gradient norm of 0.001 kcal/mol, followed by a MOPAC (AM1) full geometry optimization. The optimized geometries were subjected to density functional theory (DFT) computation with a hybrid functional B3LYP with a 6-311G**$^{++}$ basis set. The constraints charge electrostatic

* Corresponding author. Telephone: 1-630-881-1745. Fax: 1-630-904-5501. E-Mail: jasbir@jasinds.com.
† deCODE Chemistry Incorporated, 2501 Davey Road, Woodridge, Illinois 60517.
‡ Current Affiliation: Angion Biomedica Corporation, 1050 Stewart Avenue, Garden City, New York 11530. E-mail: rmishra@angion.com.
§ Current Affiliation: Jasin Discovery Solutions, Incorporated. 1156 Cordula Circle, Naperville, IL 60564. E-mail: jasbir@jasinds.com.
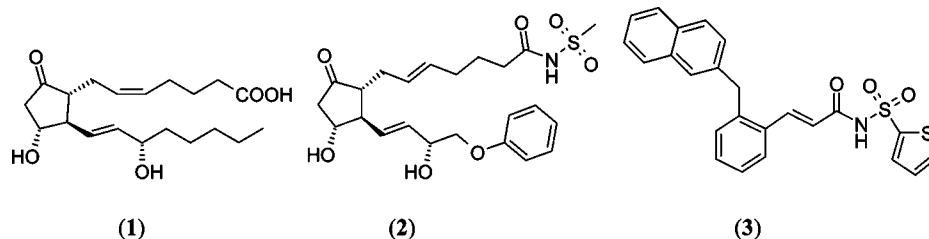
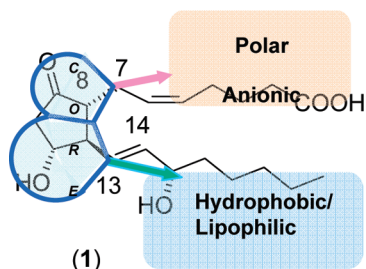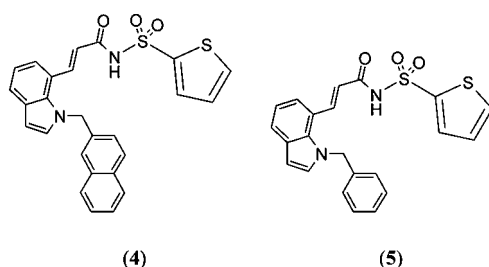**Figure 1.** (**1**) PGE2, (**2**) Sulprostone, (**3**) Merck−Frosst EP3 Antagonist.



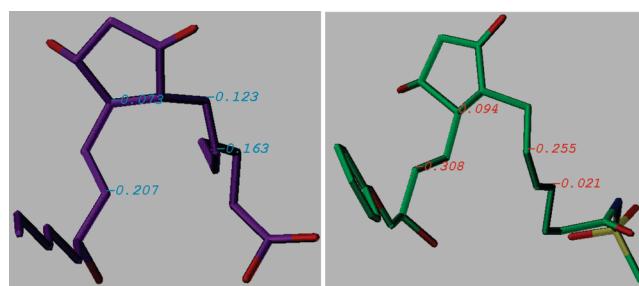**Figure 2.** Graphic representation of the approach for de novo design of new chemotypes.



| | | |
|---|---|---|
| hEP3 (binding assay, IC50): | 5.2 nM | 98 nM |
| hEP3 (CHO Cells, IC50): | 4 nM | 119 nM |

**Figure 3.** Initial indole-based hEP3 antagonist hits and corresponding activity in the receptor-binding and functional (CHO) cell-based assays, respectively.[4]
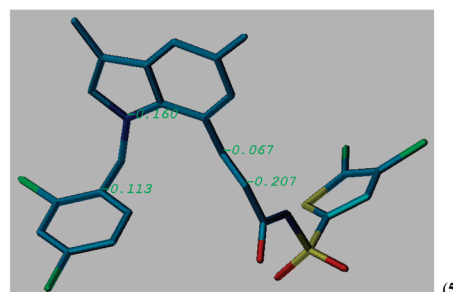


**Figure 4.** DFT minimized structures with the charges in esu for PGE2, Sulprostone, and deCODE hEP3 antagonist **5**.
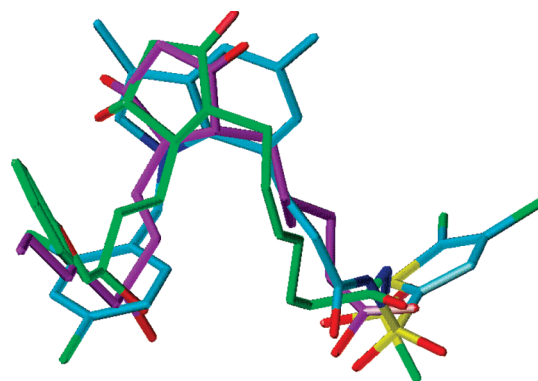


**Figure 5.** ESI alignment of PGE2 (violet), Sulprostone (green), and compound **5** (cyan).

potential gradient (CHELPG) and dipole moment were utilized. Electrostatic similarity index[9] (ESI) approach was used to align the PGE2, Sulprostone, and EP3 antagonist **5**. The alignment, based on electrostatic charge similarity,[10] showed that C7 and C13 of PGE2 matched with the indole C7- and N-benzylic carbons of the antagonist **5**, respectively (Figure 4). The ESI-based overlay of PGE2, Sulprostone, and deCODE hEP3 antagonist **5** (Figure 5) thus lend support to our initial notion of overlap for the important pharmacophoric regions of the peribicyclic core-derived analogs with the known ligands **2** and **3**.

At the outset, when we envisioned the initial design of peribicyclic core-based analogs, we postulated that a significant structural variation should be feasible for the bicyclic core portion as long as the key pharmacophoric features: (i) hydrophobic tail (Ar[1]) and (ii) polar site are retained (Figure 6a). Therefore, in order to substantiate this notion, a number of additional bicyclic cores were considered. Several bicyclic cores (Figure 6d) were selected to probe geometric constrains (Figure 6b and c) to help construct robust pharmacophore model(s). A number of bicyclic cores synthesized (representative examples are shown in Figure 6d) were minimized using MMFF94 with a gradient norm of 0.001 kcal/mol, followed by MOPAC-AM1 geometry optimization. Based on the minimized structures, the bicyclic cores selected would allow evaluation of the distance and angular tolerance limits of 2.82−3.16 Å and 122.8−131.5°, respectively.

A number of analogs with focus on variation at the bicyclic core portion and relatively small variations at the putative pharmacophoric appendages (S[1]/Ar[1] and S[2]/Ar[2]) were prepared, and IC50 for each analog using the receptor binding assay[4] was determined. This experimental data (Supporting Information, Table ST1), provides a good support to our hypothesis that the peribicyclic-derived analogs provide potent hEP3 receptor antagonists.

## PHARMACOPHORE MODEL (HYPOGEN)

HypoGen algorithm implemented in Catalyst 4.6 (Accelrys software)[11] was used for the generation of three-dimensional (3D) pharmacophore models for EP3 antagonists. A survey
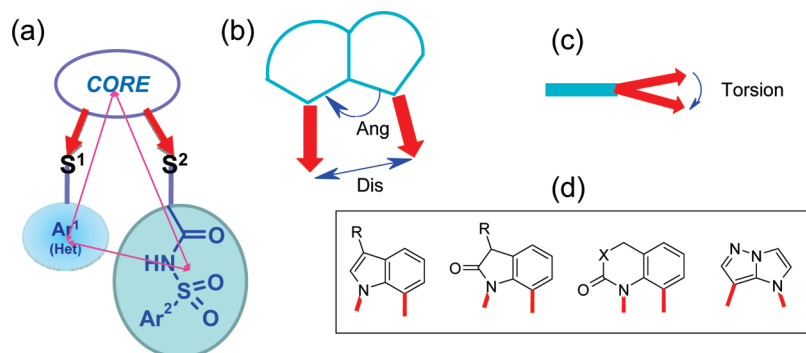
**Figure 6.** (a) Schematic of the perisubstituted ligands. (b) and (c) Represents the tolerance of the preferred geometry, and (d) shows representative examples of bicyclic cores included to help define the tolerance of geometric parameters.
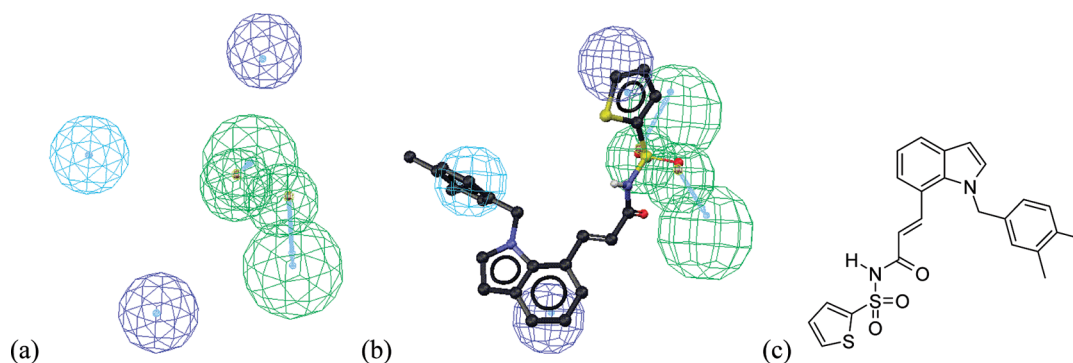


**Figure 7.** (a) Five feature pharmacophore **P5H,** (b) training set compound **17** displayed with the pharmacophore **P5H**, and (c) structure of compound **17** (training set). Color code: HBA (green); hydrophobic, Hy (blue); and hydrophobic aromatic, HyAr (cyan).

of published literature revealed many examples for successful applications of Catalyst as a useful tool for the discovery of new leads for diverse pharmacological targets.[12,13] Nineteen analogs (Supporting Information, Table ST1), with $IC_{50}$ range 0.003 to 9.425 $\mu$M, were selected for pharmacophore model generation. The procedure prescribed in Catalyst[14−16] was used for the generation of low-energy conformations of each ligand in the training set, and subsequently, the HypoGen algorithm[17,18] was employed. After completion of the HypoGen, 10 low-cost, 5 feature pharmacophores (Run-1) were obtained. Figure 7 displays the best hypothesis labeled **P5H** that was generated through the Run-1. Since Catalyst does not consider the acylsulphonamide function ($pK_a \sim 6−8$) as a negative ionizable functionality, no hypothesis with negatively ionized (NI) feature was obtained. Therefore, 'Exclude/Or Quick Tool' and a script for NI representing acylsulphonamide were implemented for HypoGen to recognize the acylsulphonamide feature as an acid (mimetic) functionality. After incorporating these modifications, we obtained a second set of 10 best, low-cost hypotheses that included the NI feature (Run-2). The best hypothesis labeled: **P5N**, from this second HypoGen run (Run-2) is shown in Figure 8. The essential difference (Table 1) between these two hypotheses, **P5H** and **P5N**, being hydrogen-bond acceptor (HBA) and NI as the fifth feature, respectively. The other four features are identical for the two HypoGen runs (**P5H** and **P5N**).

### EVALUATION AND ANALYSIS OF HYPOGEN MODELS

The evaluation of the two hypotheses **P5H** and **P5N** was performed based on cost analysis, score hypothesis, and Fisher test. The hypothesis **P5N** had a 'Config' value of 17.28 which indicated that some of the hypotheses might
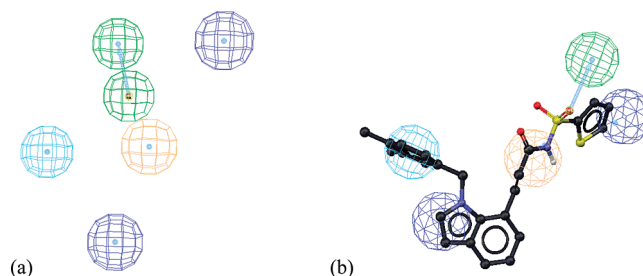


**Figure 8.** (a) Five feature Pharmacophore **P5N**, (b) training set compound **17** displayed with the P5N pharmacophore. Color code: HBA (green), Hy (blue), HyAr (cyan), and NI (brown).

have been excluded during the optimization step, as the acceptance value should have been ≤17.00. Also, the differences in the cost to null values were 51 and 44 bits for **P5H** and **P5N** pharmacophores, respectively. These indicate that both of these hypotheses have high probability of representing 75−90% of true correlation in the data set. Since, the 'Config' and the cost difference were too close in both hypotheses, the Fisher test was performed to explore the possibility of a chance correlation in both the models. The catScramble program implemented in Catalyst was used to generate 19 random spread sheets, and HypoGen was run using the best hypothesis from Run-1 (**P5H**) and Run-2 (**P5N**) with a 95% confidence level.[19] It is interesting to note that the **P5H** hypothesis provided a best correlation of 0.72 with a root-mean square (rms) of 1.64, which was not close to the best results obtained through the initial run (see Table 1). Whereas, for the second hypothesis, **P5N**, a correlation of 0.75 with a rms of 1.62 was obtained, and these values are very close to the values obtained in the initial run (Table 1). The scrambling test results raised questions about the validity of the **P5N** hypothesis. Finally, both the hypotheses

EP3 ANTAGONIST PHARMACOPHORE MODEL

*J. Chem. Inf. Model., Vol. 50, No. 8, 2010* **1505**

**Table 1.** Statistical Data Comparing Differences between the Best Hypotheses Obtained from Two HypoGen Runs

| best hypothesis | total cost | fixed cost | null cost | config | rms | correlation features | features represented in hypothesis |
|---|---|---|---|---|---|---|---|
| P5H | 86.45 | 79.33 | 137.41 | 14.29 | 1.04 | 0.82 | HBA, HBA, HyAr, Hy, Hy |
| P5N | 93.30 | 81.95 | 137.41 | 17.28 | 1.50 | 0.77 | HBA, NI, HyAr, Hy, Hy |

were used to score training set compounds. These predicted $IC_{50}$ values are shown in the Supporting Information, Table ST1. Except for a couple of very active compounds, **P5H** was able to predict within two- to six-fold of the observed values; on the other hand, **P5N** consistently gave poor predictions. This result further indicated that the **P5N** hypothesis is not suitable for further improvement.

## CUSTOMIZING THE HYPOTHESIS THROUGH MERGE FEATURE

HypoGen is limited to generation of a maximum of five-feature pharmacophore model(s). Therefore, for building pharmacophore models which contains more than five features, one needs to generate and merge additional features to the existing hypothesis.[11] From our structure—activity relationship (SAR) data, we were aware that the acylsulphonamide is an essential pharmacophoric feature, as replacement of $-CONHSO_2-$ with $-CON(CH_3)SO_2-$ leads to a loss in $hEP_3$ binding activity (data not shown). Catalyst defines hydrogen-bond donor (HBD) as a vector, where as NI represents a point pharmacophoric feature. This would imply that the hydrogen of the $-CONHSO_2-$ may behave as HBD, i.e., a vector, rather than as a point feature. Hypothesis **P5H** has two HBA but no HBD or NI. In order to map a new feature "HBD", one of the active analogs from the training set (compound 17) was considered, and the vector feature generated. The new HBD feature was finally merged into the **P5H** hypothesis making it a six-feature pharmacophore model, labeled as **P6** (Figure 9).

## REGRESS HYPOTHESIS

Since based on our SAR information we added one extra feature to the hypothesis, it needed to be regressed before the score or computation of the predictive $IC_{50}$ values could be performed. With the addition of sixth feature in the form of HBD and regressing, the correlation was improved from 0.82 to 0.89 for the training set compounds. The new six-feature hypothesis **P6** was also tested using the catScramble program and the Fisher test procedure, as mentioned before, while evaluating the **P5H** and **P5N** models. The best correlation obtained for **P6** in the catScramble test was found to be 0.75.
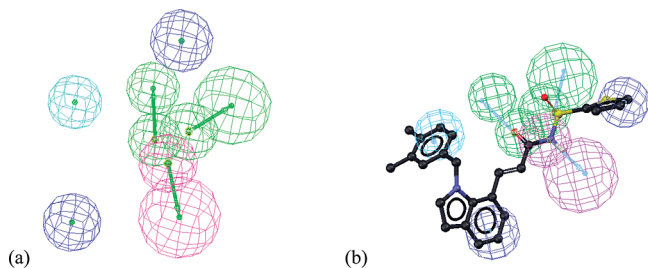


**Figure 9.** Six-feature, regressed pharmacophore **P6** with training set compound **17**. Color code: HBA (green), Hy (blue), HyAr (cyan), and HBD (magenta).

## VALIDATION OF THE HYPOTHESIS

The primary idea of building a quantitative model is to identify the active structures that allow one to forecast their activity as accurately as possible.[13] This validation was carried out using a test set of 11 distinct compounds (T1—T11, Table 2) that contain features present in the initial training set. The biological activities ($IC_{50}$ values) for the test set compounds were predicted using **P5H** and **P6** models, respectively. As shown in Tables 2 and 3, the **P6** hypothesis truly translated the SAR into evocative chemical information. Further analysis of the data presented in Table 3 reveals that the energy of the mapping conformers for the entire test set of compounds for the regressed hypothesis **P6** was in the acceptable range.[11] Analysis of the results for diverse series of compounds in Table 3 and 4 reveals that activity of essentially all test set compounds was predicted well, providing calculated $IC_{50}$ values that are within three-fold of the corresponding experimental values and have energy for the conformation chosen to be <8 kcal/mol.[20] The predictive power of this customized **P6** model increased compared to the original **P5H** model. The square of the correlation coefficients ($R^2$) between the observed and calculated values for the test set increased from 0.82 to 0.90. We believe that by incorporating the extra HBD feature, the predictive ability of the **P6** increased, corroborating the observed SAR analysis. The analysis of the performance of these various pharmacophores, as represented graphically in Figure 9a, clearly shows **P6** to be a superior model.

## EXTENSION OF THE PHARMACOPHORE P6 TO DIVERSE CHEMOTYPES

As postulated, a significant extent of structural variations at the central bicyclic core was projected to be tolerated as long as the core retained the overall hydrophobic characteristics and allowed for maintaining the proper spatial orientation and positioning of the key binding elements, "namely the polar acidic and lipophilic tails" in a U-shaped trajectory. Based on this hypothesis, right from the start, we had elected to designate the core as hydrophobic 'Hy' and not as a 'HyAr' (hydrophobic aromatic) pharmacophoric feature. Therefore, we decided to modify the bicyclic core of the targeted molecules retaining hydrophobic characteristics to reduce overall planarity of the ligand and the potential ligand—ligand $\pi$-stacking, focusing on nonaromatic heterocyclic cores. We reasoned that the resulting molecules are likely to possess favorable physicochemical properties including better aqueous solubility.[21] We elected to focus on the [4.3.0] bicyclic system represented by the saturated indolone as core.[21] The regressed hypothesis **P6** was thus extended to evaluate molecules containing a saturated core as shown in the Figure 10. Six compounds (T12—T17),

**Table 2.** Structures of the Test Set Compounds (T1−T11) for Validating Pharmacophore Models
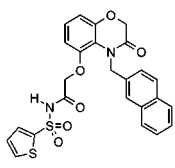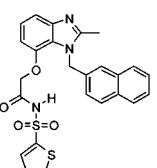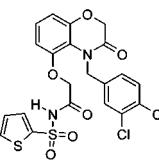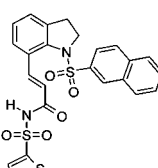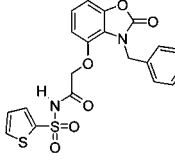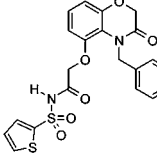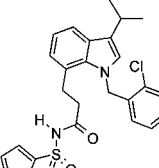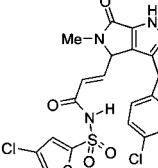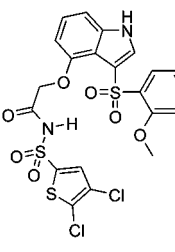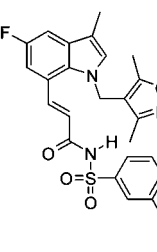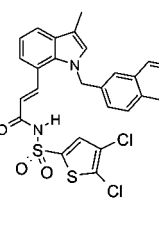


**Table 3.** Predicted $IC_{50}$ Values along with Energy of the Respective Mapped Conformer for Test Set of Compounds[a]

| compound | $IC_{50}$-obs (nM) | predicted $IC_{50}$ using **P5H** (nM) | energy of mapped conformer (kcal/mol) | predicted $IC_{50}$ using **P5N** (nM) | energy of mapped conformer (kcal/mol) | predicted $IC_{50}$ using **P6** (nM) | energy of mapped conformer (kcal/mol) |
|---|---|---|---|---|---|---|---|
| T1 | 3458.8 | 1900.0 | 0.416 | 950.0 | 12.64 | 3900.0 | 4.46 |
| T2 | 1760.0 | 330.0 | 8.58 | 530.0 | 18.99 | 1340.0 | 5.86 |
| T3 | 454.3 | 310.0 | 9.2 | 64.0 | 4.69 | 590.0 | 5.96 |
| T4 | 35.8 | 74.0 | 10.48 | 1600.0 | 9.12 | 19.0 | 6.72 |
| T5 | 2799.9 | 590.0 | 9.30 | 21.0 | 9.84 | 1500.0 | 8.26 |
| T6 | 6876.0 | 2240.0 | 14.15 | 190.0 | 11.72 | 7380.0 | 7.24 |
| T7 | 1312.5 | 100.0 | 16.93 | 450.0 | 18.69 | 1100.0 | 5.92 |
| T8 | 1777.7 | 89.0 | 3.91 | 13.0 | 3.79 | 33.0 | 11.23 |
| T9 | 7.5 | 51.0 | 1.75 | 48.0 | 9.91 | 14.0 | 8.22 |
| T10 | 14.5 | 42.0 | 7.39 | 87.0 | 5.60 | 17.0 | 7.23 |
| T11 | 2.0 | 63.0 | 3.66 | 80.0 | 6.54 | 6.1 | 6.29 |

[a] As obtained using different pharmacophore hypotheses.

with variations in the $Ar^1$ and $Ar^2$ portion, were considered and scored using **P6** (Table 4). We were gratified to find that the predicted values of the compounds were within two-three folds of the experimental values for this series of analogs.

Although, the acylsulphonamide is considered as an acid mimetic, as described above, inclusion of the acylsulphonamide NH as HBD (vector) rather than NI (single point) resulted in a superior pharmacophore model. Therefore, we envisioned that other functional groups which contain this HBD feature should provide viable functional group replacements. During the new analog generation, we confirmed that simple modification of the acylsulphonamide ($-CO-NH-SO_2-$) to either an amide ($-CO-NH-$) or a sulphonamide ($-CH_2-NH-SO_2-$) resulted in loss in $hEP_3$ affinity (data

not shown). It is worth noting that the carbonyl group of the acylsulphonamide group was mapped as HBA in the model **P6**. Therefore, we postulated that replacement of the $-C=C-C=O-$ functionality with a heterocyclic mimetic which contain a heteroatom, capable of serving as HBA, proximal to the sulphonamide NH might serve as an appropriate functional replacement to provide analogs with good affinity for $EP_3$ receptor and would be expected to behave as full antagonists. Such structural modifications utilizing heterocycles as $-CH=CH-C=O-$ mimetic (Figure 11) would also lead to a more rigid linker replacement. To our gratification, an initial analog representing this structural variation provided a very potent compound **6** ($IC_{50}$ = 4.2 nM). The series has thus been extended to include additional heterocycles,[22] and the pharmacophore model **P6** has been

**Table 4.** Predictive $IC_{50}$ Values Computed Using **P6** Pharmacophore Model for Analogs T12–T17 and T18–T23[a]

| Compound | Structure | Obs_IC50 (nM) | Predicted_IC50 using P6 (nM) | Energy of mapping conformer (kcal/mol) | Compound | Structure | Obs_IC50 (nM) | Predicted_IC50 using P6 (nM) | Energy of mapping conformer (kcal/mol) |
|---|---|---|---|---|---|---|---|---|---|
| T12 | (structure) | 13.4 | 50.3 | 4.87 | T18 | (structure) | 2576 | 5500 | 0.98 |
| T13 | (structure) | 57.2 | 76.2 | 8.03 | T19 | (structure) | 2.2 | 3.6 | 3.60 |
| T14 | (structure) | 15.2 | 51.5 | 6.67 | T20 | (structure) | 1978.1 | 667.0 | 6.95 |
| T15 | (structure) | 84.1 | 65.2 | 4.31 | T21 | (structure) | 59.4 | 42.0 | 7.11 |
| T16 | (structure) | 12.9 | 42.0 | 8.61 | T22 | (structure) | 23.7 | 14.0 | 6.57 |
| T17 | (structure) | 9.8 | 24.6 | 7.47 | T23 | (structure) | 88.3 | 190.0 | 5.76 |

[a] Derived from new chemotype-saturated bicyclic and heterocyclic–bicyclic cores, respectively.

shown to be extendable to this new chemotype as well (Table 4). The chosen spacing parameter of 5 pm has been able to correctly map the contiguous features: HBA, HBD, and HBA on to these heterocyclic classes of molecules and to diverse chemotypes representing active EP₃ antagonists, presented here.

## CONCLUSION

The initial premise for the design of peribicyclic analogs conceived through chemical insight was supported by use of electrostatic similarity index (ESI) approach. The preliminary data set based on a core variation hypothesis provided an initial set, which gave an incentive to generate two five-feature pharmacophore models, **P5H** and **P5N**. The initial five-feature model **P5H** was merged with an additional hydrogen-bond donor (HBD) as a vector pharmacophoric feature, describing the acylsulphonamide. Following a linear regression, the six-fetaure pharmacophore model **P6** was shown to provide good predictability of $IC_{50}$ values ($R^2 = 0.90$) for the test set of compounds. The refined **P6** model subsequently supported bicyclic core variations allowing chemotype diversification to include saturated bicyclic and heteroaryl peribicyclic derived analogs. These series of analogs have been demonstrated to provide potent isoform selective hEP₃ antagonists. Overall, iterative cycles utilizing pharmacophore generation and its use as predicted tools aided for generation of perisubstituted bicyclics as novel chemotypes leading to generation of potent hEP₃ antagonists with drug-like properties.

## Comparision of hEP₃ IC₅₀ Values Predicted Using Three Pharmacophore Models vs. Experimental Values
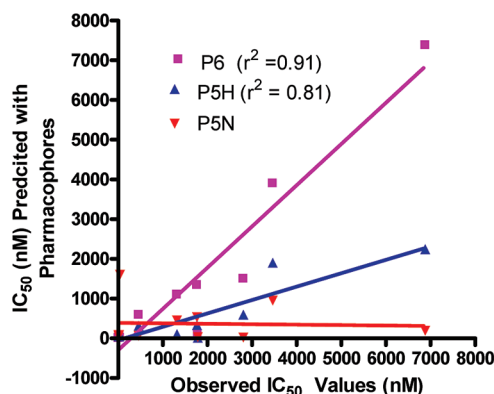


**Figure 10.** Scatter plot showing comparison of the three predicted IC₅₀ values obtained from **P5H**, **P5N**, and **P6** versus the experimental value.
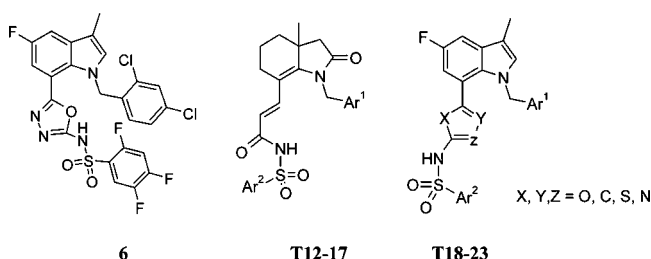


**Figure 11.** New chemotypes, T12−T17 and T18−T23, extended analogs that fit **P6** model.

## ACKNOWLEDGMENT

**Supporting Information Available:** Pages S1−S6. Table ST1 contains a training set of compounds with observed and predicted IC₅₀ from Run-1 and Run-2 along with error factor. This material is available free of charge via the Internet at http://pubs.acs.org.

## REFERENCES AND NOTES

(1) (a) Abramovitz, M.; Adam, A.; Boie, Y.; Godbout, C.; Lamontagne, S.; Rochette, C.; Sawyer, N.; Tremblay, N. M.; Belley, M.; Gallant, M.; Dufresne, C.; Gareau, Y.; Ruel, R.; Juteau, H.; Labelle, M. The utilization of recombinant prostanoid receptors to determine the affinities and selectivities of prostaglandins and related analogs. *Biochim. Biophys. Acta* **2000**, *1483*, 285–293. (b) Kiriyama, A.; Ushukubi, K.; Kobayashi, T.; Hirata, M.; Sugimoto, Y.; Narumiya, S. Ligand binding specificities of the eight types and subtypes of the mouse prostanoid receptors expressed in Chinese hamster ovary cells. *Br. J. Pharmacol.* **1997**, *122*, 217–224.

(2) Gross, S.; Tilly, P.; Hentsch, D.; Vonesch, J. L.; Fabre, J. E. Vascular wall-produced prostaglandin E2 exacerbates arterial thrombosis and atherothrombosis through platelet EP3 receptors. *J. Exp. Med.* **2007**, *204*, 311–320.

(3) Fabre, J.; Nguyen, M.; Athirakul, K.; Coggins, K.; McNeish, J. D.; Austin, S.; Parise, L. K.; FitzGerald, G. A.; Coffman, T. M.; Koller, B. H. Activation of the murine EP3 receptor for PGE₂ inhibits cAMP production and promotes platelet aggregation. *J. Clin. Invest.* **2001**, *107*, 603–610.

(4) Singh, J.; Zeller, W.; Zhou, N.; Hategen, G.; Mishra, R.; Polozov, A.; Yu, P.; Onua, E.; Zhang, J.; Zembower, D.; Kiselyov, A.; Ramírez, J.; Sigthorsson, G.; Bjornsson, J.; Thorsteinnsdottir, M.; Andrésson, T.; Bjarnadottir, M.; Magnusson, O.; Stefansson, K.; Gurney, M. Antagonists of The EP3 Receptor for Prostaglandin E2 Are Novel Anti-Platelet Agents That Do Not Prolong Bleeding. *ACS Chem. Biol.* **2009**, *4* (2), 115–126.

(5) Lavrador, K.; Murphy, B.; Saunders, J.; Struthers, S.; Wang, X.; Williams, J. A Screening Library for Peptide Activated G-Protein Coupled Receptors. *J. Med. Chem.* **2004**, *47* (27), 6864–6874.

(6) Bondensgaard, K.; Ankersen, M.; Thogersen, H.; Hansen, B. S.; Wulff, B. S. Recongnition of Privileged Structures by G-Protein Coupled Receptors. *J. Med. Chem.* **2004**, *47* (4), 888–899.

(7) Costanzi, S. On the Applicability of GPCR Homology Models to Computer-Aided Drug Discovery: A Comparison between In Silico and Crystal Structures of the $\beta_2$-Adrenergic Receptor. *J. Med. Chem.* **2008**, *51* (10), 2907–2914.

(8) Juteau, H.; Gareau, Y.; Labelle, M.; Sturino, C. F.; Sawyer, N.; Tremblay, N.; Lamontagne, S.; Carriere, M.; Denis, D.; Metters, K. M. Structure-Activity Relationship of Cinnamic Acylsulphonamide on Human EP3 Prostanoid Repector. *Bioorg. Med. Chem. Lett.* **2001**, *9*, 1977–1984.

(9) Girones, X.; Amat, L.; Carbo-Dorca, R. Using Molecular Quantum Similarity Measures as Descriptors in Quantitative Structure-Toxicity Relationships. *SAR QSAR Environ. Res.* **1999**, *10*, 545–556.

(10) Burt, C.; Richards, W. G.; Huxley, P. The Application of Molecular Similarity Calculations. *J. Comput. Chem.* **1990**, *11*, 1139–1146, and references therein.

(11) *Catalyst Manual*, version 4.6; Accelrys Inc.: San Diego, CA, 2004.

(12) (a) Krovat, E. M.; Langer, T. Non-Peptide Angiotensin II Receptor Antagonists: Chemical Feature Based Pharmacophore Identification. *J. Med. Chem.* **2003**, *46*, 716–726. (b) Debnath, A. K. Pharmacophore Mapping of a Series of 2,4-Diamino-5-deazapteridine Inhibitors of Mycobacterium Avium Complex Dihydrofolate Reductase. *J. Med. Chem.* **2002**, *45*, 41–53. (c) Karki, R. G.; Kulkarni, M. V. A Feature Based Pharmacophore for Candida Albicans MyristoylCoA: Protein N-Myristoyltransferase Inhibitors. *Eur. J. Med. Chem.* **2001**, *36*, 147–163. (d) Hirashima, A.; Pan, C.; Kuwano, E.; Taniguchi, E.; Eto, M. Three-Dimensional Pharmacophore Hypotheses for the Locust Neuronal Octopamine Receptor (OAR3). Part 2: Agonists. *Bioorg. Med. Chem.* **1997**, *40*, 4103–4112. (e) Lopez-Rodriguez, M.; Porras, E.; Benhamu, B.; Ramos, J. A.; Morcilla, M. J. First Pharmacophoric Hypothesis for 5HT-7 Antagonism. *Bioorg. Med. Chem. Lett.* **2000**, *10*, 1097–1100. (f) Singh, J.; van Vlijmen, J.; Liao, Y.; Lee, W.; Cornebise, M.; Harris, M.; Shu, I.; Gill, A.; Cuervo, J.; Abraham, W. M.; Adams, S. P. Identification of Potent and Novel α4β1 Antagonists Using *in Silico* Screening. *J. Med. Chem.* **2002**, *45*, 2988–2993. (g) Palomer, A.; Cabre, F.; Pascual, J.; Campos, J.; Trujillo, M. A.; Entrena, A.; Gallo, M. A.; Garcia, L.; Mauleon, D.; Espinosa, A. Identification of Novel Cyclooxygenase-2 Selective Inhibitors Using Pharmacophore Models. *J. Med. Chem.* **2002**, *45*, 1402–1411. (h) Kurogi, Y.; Miyata, K.; Okamura, T.; Hashimoto, K.; Tsutsumi, K.; Nasu, M.; Moriyasu, M. Discovery of Novel Mesangial Cell Proliferation Inhibitors Using a Three-Dimensional Database Searching Method. *J. Med. Chem.* **2001**, *44*, 2304–2307.

(13) Funk, O. F.; Kettmann, V.; Drimal, J.; Langer, T. Chemical Function Based Pharmacophore Generation of Endothelin-A Selective Receptor Antagonists. *J. Med. Chem.* **2004**, *47*, 2750–2760.

(14) The 3D structures of the compounds had been generated using Catalyst 2D/3D sketcher. Applying the 'best quality' conformational search option and using the threshold energy of 20 kcal/mol, the conformations for all 19 structures were generated. These selected compounds show activity range within 4 log orders of magnitude. Catalyst conformational search utilized CHARMM force field parameters (see ref 15) and a Poling technique (see ref 16) to ensure conformational variations are within the accessible space by penalizing a newly generated conformer if it is too similar to any other conformer.

(15) Brooks, B. R.; Brucolleri, R. E.; Olafson, B. D.; States, D. J.; Swaminathan, S. CHARM: A program for Macromolecular Energy Minimization and Dynamic Calculations. *J. Comput. Chem.* **1983**, *4*, 187–217.

(16) Smellie, A.; Teig, S. L.; Towbin, P. Poling: Promoting Conformational Coverage. *J. Comput. Chem.* **1995**, *16*, 171–187.

(17) HypoGen proceeds through three different steps: (i) *constructive phase* where pharmacophores that are common among the most active compounds are elaborated; (ii) *subtractive phase* where pharmacophores that fit the inactive member of the training set are removed; and (iii) *optimization phase* where the remaining hypotheses are refined. Each perturbation is evaluated through the cost of errors, the configuration, and the weight cost. The program by default generates the 10 best hypotheses with the lowest cost in the output file.

(18) The "catHypo.forceAbsolute Stereochemistry" parameter was set to unity to force the hypothesis algorithm to consider only the

EP3 ANTAGONIST PHARMACOPHORE MODEL

*J. Chem. Inf. Model., Vol. 50, No. 8, 2010* **1509**

supplied configuration with no enantiomers or diastereomers variations being allowed. The uncertainty of the compound's activity was set to 3 (HypoGen default value). The hydrophobic (Hy), ring aromatic (RA), hydrogen-bond donor (HBD), hydrogen-bond acceptor (HBA), and negative ionizable (NI) features for compounds in the training set along with default 'min/max' and the excluded volume functionality using HypoRefine were selected for generation of pharmacophore models. The spacing parameter was set to 5, which enabled the program to consider the features with a minimum of 5 pm as two distinct features. The remaining parameters were set to the default values.

might be the bioactive form, the low-energy tautomer was selected for the analysis. As shown in the Table 3, this tautomer gave ~50-fold difference in calculated vs. experimental value for this compound and a conformational energy of 11.23 kcal/mol.

(19) Du, Lu-Pei.; Tsai, K.; Li, M.; You, Q.; Xia, L. The Pharmacophore Hypothese of $I_{kr}$ Potassium Channel Blockers: Novel Class III Antiarrhythmic Agents. *Bioorg. Med. Chem. Lett.* **2004**, *14*, 47771–47777.

(20) Compound T8 could potentially exist in multiple tautomeric forms and since it is not feasible to determine experimentally which tautomer

(21) O'Connell, M.; Zeller, W.; Burgeson, J.; Mishra, R. K.; Ramirez, J.; Kiselyov, A. S.; Andrésson, T.; Gurney, M. E.; Singh, J. Peri-substituted hexahydro-indolones as novel, potent and selective human EP3 receptor antagonists. *Bioorg. Med. Chem. Lett.* **2009**, *19* (3), 778–782.

(22) Hategan, G.; Polozov, A. M.; Zeller, W.; Cao, H.; Mishra, R. K.; Kiselyov, A. S.; Ramirez, J.; Halldorsdottir, G.; Andrésson, T.; Gurney, M. E.; Singh, J. Heterocyclic 1,7-Disubstituted Indole Sulphonamides Are Potent and Selective Human EP3 Receptor Antagonists. *Bioorg. Med. Chem. Lett.* **2009**, *19* (23), 6797–6800.

CI100003Q